

Atomic Partitioning of the Dissociation Energy of the P–O(H) Bond in Hydrogen Phosphate Anion (HPO₄²⁻): Disentangling the Effect of Mg²⁺

Chérif F. Matta,^{*,†,‡} Alya A. Arabi,[†] and Todd A. Keith^{*,§}

Department of Chemistry and Physics, Mount Saint Vincent University, Halifax, Nova Scotia, Canada B3M 2J6, Department of Chemistry, Dalhousie University, Halifax, Nova Scotia, Canada B3H 4J3, and Department of Chemistry, University of Missouri–Kansas City, 5110 Rockhill Road, Kansas City, Missouri 64110

Received: May 9, 2007; In Final Form: June 19, 2007

This paper has three goals: (1) to provide a first step in understanding the atomic basis of the role of magnesium in facilitating the dissociation of the P–O bond in phosphorylated biochemical fuel molecules (such as ATP or GTP), (2) to compare second-order Møller–Plesset perturbation theory (MP2) results with those obtained at the more economical density functional theory (DFT) level for a future study of larger more realistic models of ATP/GTP, and (3) to examine the calculation of atomic total energies from atomic kinetic energies within a Kohn–Sham implementation of DFT, as compared to ab initio methods. A newly described method based on the quantum theory of atoms in molecules (QTAIM), which is termed the “atomic partitioning of the bond dissociation energy” (APBDE), is applied to a simple model of phosphorylated biological molecules (HPO₄²⁻). The APBDE approach is applied in the presence and in the absence of magnesium. It is found that the P–O(H) bond in the magnesium complex is shorter, exhibits a higher stretching frequency, and has a higher electron density at the bond critical point than in the magnesium-free hydrogen phosphate anion. Though these data would seem to suggest a stronger P–O(H) bond in the magnesium complex compared to the magnesium-free case, the homolytic breaking of the P–O(H) bond in the complex is found to be easier, i.e., has a lower BDE. This effect is the result of the balance of several atomic contributions to the BDE induced by the magnesium cation, which stabilizes the dissociation product more than it stabilizes the intact model molecule.

Introduction

Chemical reactions involve bond making and breaking, processes that are thermodynamically driven by the relative strengths of the chemical bonds in the reactants and products. A fundamental property that measures the strength of a chemical bond is the bond dissociation energy (BDE),^{1–4} defined in terms of the enthalpy of the bond dissociation reactions:⁵



Defined in this manner, the BDE can be indirectly measured experimentally as the difference between the sum of the heats of formation of the products and the corresponding sum for the reactant, that is

$$\text{BDE}(\text{R-X}) \equiv \Delta H^\circ(\text{R-X}) = \Delta H_f^\circ(\text{R}^\bullet) + \Delta H_f^\circ(\text{X}^\bullet) - \Delta H_f^\circ(\text{R-X}) \quad (2)$$

Equation 2 expresses the BDE, which characterizes a *particular* bond, a local property, in terms of “global” properties of the reactant and products, namely, the heats of formation.

Recently, a new method was proposed within the framework of the quantum theory of atoms in molecules (QTAIM)^{6–8} to trace the local (atomic) contributions to the electronic part of

the BDE (the dominant part). The new approach, which we term the “atomic partitioning of the bond dissociation energy”, or APBDE, was applied to a series of alkanes and alkenes.⁹ In this approach, the vibrationless 0 K electronic BDE is expressed as the sum of atomic contributions:

$$\text{BDE}_{\text{electronic}(0\text{K})} = \sum_{\Omega} \Delta E(\Omega)_{\text{BDE}} \quad (3)$$

where each atomic contribution to the BDE consists of the change in the energy of the atom accompanying the breaking of the particular bond of interest [$\Delta E(\Omega)$], and where the sum runs over all the atoms in the molecule. In this scheme, an individual atomic contribution is defined as

$$\Delta E(\Omega)_{\text{BDE}} = E(\Omega)_{\text{products}} - E(\Omega)_{\text{reactant}} \quad (4)$$

where $E(\Omega)_{\text{reactant}}$ is the energy of a particular atom Ω in the reactant (before bond dissociation) and $E(\Omega)_{\text{products}}$ is the energy of the same atom in the dissociation products (after bond dissociation).

This approach revealed that the two carbon atoms between which a C–C single bond is severed contribute *nothing* to the BDE due to a subtle balance of atomic energy components. Instead, it is the atoms that are directly bonded to these two carbon atoms that are destabilized most by breaking the C–C bond.⁹

Phosphorylated nucleotides such as ATP and GTP are used by living cells to store chemical energy in their so-called “high-energy phosphate bonds”. Although the dissociation of a

* Corresponding authors. C.F.M.: e-mail, cherif.matta@msvu.ca; telephone, +1-(902)-457-6142; fax, +1-(902)-457-6134. T.A.K.: e-mail, keithta@umkc.edu; telephone, +1-(913)-268-3271; fax, +1(913)-268-3445.

[†] Mount Saint Vincent University.

[‡] Dalhousie University.

[§] University of Missouri–Kansas City.

chemical bond is always an endothermic process, the dissociation of a P–O bond in the cell is always coupled with the formation of another chemical bond resulting in a net release of energy. The dissociation of the P–O bond is, thus, a necessary step for the release of free energy in the biological system, a step facilitated by the presence of divalent (and even monovalent^{10–13}) cations, particularly Mg^{2+} , as cofactors in kinase enzymes. The role of cations in facilitating the enzymatic hydrolysis of phosphorylated molecules has generated intense interest spanning several decades (see, for example, refs 10 and 14–25). The local energetic changes brought about by complexation with the magnesium ion have never been discussed, and this is what this first paper (in a series) is attempting to explore using the APBDE approach.

A simple model of a phosphorylated nucleotide is the hydrogen phosphate anion, HPO_4^{2-} , free as well as complexed with a magnesium cation (MgHPO_4). To understand and evaluate the effect of Mg^{2+} on the strength of the P–O(H) bond, the bond representing the one that is broken in kinase-catalyzed reactions, we undertook an APBDE study in the presence and in the absence of the Mg^{2+} cation. Admittedly, this model is very different from real systems (even in the gas phase) where the Mg^{2+} is likely to be complexed with two neighboring phosphate groups and at least two water molecules.²⁶ Furthermore, the biochemical rate enhancement depends on the change in the height of the barrier of the hydrolysis reaction. Our purpose in this paper is not so much to model the real biological reaction (this will be the subject of a future study) but rather to uncover the basic principles underlying the remote electronic effect(s) of Mg^{2+} on the strength of a simple model of the P–O bond. Furthermore, because of the small size of the species involved in this simple model study, a detailed comparison between MP2 and B3LYP with a large basis set was possible to validate future B3LYP calculations on much larger, more realistic, models.

Method

1. Levels of Theory and Calculation Details. Electronic structure calculations were performed using Gaussian 03²⁷ at the MP2(full)/6-311++G(d,p)//MP2(full)/6-311++G(d,p) and B3LYP/6-311++G(d,p)//B3LYP/6-311++G(d,p) levels of theory. The corresponding unrestricted formulations were employed for open-shell species in the dissociation products.

Electron densities were analyzed according to the QTAIM^{6–8} using the AIMPAC's PROAIMV^{28–30} to perform the atomic integrations. A total of 24 atomic integrations were performed with an overall average of the integrated atomic Laplacian function magnitude ($|L(\Omega)| = |(-1/4)\int_{\Omega}\nabla^2\rho(\mathbf{r})\text{d}\mathbf{r}|$) of 3.8×10^{-4} ($\pm 8.4 \times 10^{-4}$) for the MP2 calculations and 3.8×10^{-4} ($\pm 7.6 \times 10^{-4}$) in the case of the B3LYP calculations, the numbers in parentheses being the standard deviations.

2. Quality of the Geometry Optimization. Because this paper focuses on atomic energies, all wavefunctions were obtained at the same level of theory used in the geometry optimization to avoid complications in the definition of atomic energies due to nonvanishing forces on the nuclei. Furthermore, the optimizations have been carefully conducted to minimize the deviations of the final forces on the nuclei from zero. At the MP2 level, the final average root-mean-square (RMS) force per system was 1.8×10^{-6} ($\pm 1.3 \times 10^{-6}$) hartree/bohr, and the average maximum force in any single system was 4.2×10^{-6} ($\pm 2.8 \times 10^{-6}$) hartree/bohr, $n = 5$ (two closed-shell systems and three open-shell dissociation products). The corresponding values for the B3LYP calculation are 2.0×10^{-6}

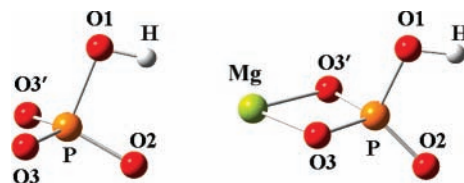


Figure 1. Numbering scheme for HPO_4^{2-} anion (left) and the $\text{Mg}-\text{HPO}_4$ complex at their MP2/6-311++G(d,p) optimized geometries.

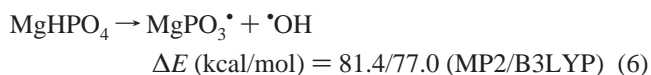
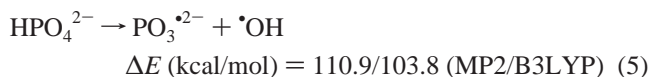
($\pm 1.7 \times 10^{-6}$) hartree/bohr for the average RMS force per system, and 4.8×10^{-6} ($\pm 3.8 \times 10^{-6}$) hartree/bohr for the average maximum force in any single system.

3. Spin Contamination. Spin contamination was found to be insignificant in all the unrestricted calculations with the expectation value $\langle S^2 \rangle$ deviating by less than 0.8% from the ideal value of 0.75 for the doublet state. In the case of the spin unrestricted MP2 (UMP2) open-shell calculations, $\langle S^2 \rangle$ was 0.7538 for $\text{PO}_3^{\bullet 2-}$, 0.7503 for $\text{Mg}-\text{PO}_3^{\bullet}$, and 0.7558 for $\bullet\text{OH}$. The corresponding values for the spin unrestricted B3LYP (UB3LYP) calculations were 0.7518 for $\text{PO}_3^{\bullet 2-}$, 0.7502 for $\text{Mg}-\text{PO}_3^{\bullet}$, and 0.7522 for $\bullet\text{OH}$.

Results and Discussion

Figure 1 displays ball-and-stick models of the optimized geometries of the two parent systems, HPO_4^{2-} and its magnesium complex $\text{Mg}-\text{HPO}_4$, along with the numbering scheme. To understand the role of Mg^{2+} in the dissociation of the P–O1 bond, four comparisons of atomic and bond properties will be made within each level of theory: a comparison between the properties of each system before and after bond dissociation and a comparison of the effect of the complexation with magnesium on the reactants and on products. All along, we will also compare the results from the MP2 and B3LYP calculations to assess the performance of B3LYP against MP2 especially with regards to the atomic energies. We will often refer to the two levels as $n_{\text{MP2}}/n_{\text{B3LYP}}$ (the values before and after the slash referring to the MP2 and the B3LYP values, respectively). When only one numerical result is quoted, that result belongs to the MP2 calculation.

1. Global Energy Changes upon the Dissociation of the P–O1 bond. Mg^{2+} significantly reduces the BDE of the P–O1 bond [by 29.5/26.8 kcal/mol (MP2/B3LYP)], as can be seen from the enthalpy changes of the following reactions:



In the above reactions, B3LYP predicts lower BDEs than MP2 (7.1 kcal/mol in eq 5 and 4.4 kcal/mol in eq 6), but this difference is small relative to the difference in BDE between the two reactions.

Accompanying the lower BDE of the P–O1 bond in the magnesium complex (compared to the free HPO_4^{2-} anion) is a significantly shortening of the bond, a higher electron density at the bond critical point (BCP), and a higher stretching frequency. In the case of free HPO_4^{2-} the P–O1 bond length is 1.772/1.787 Å, ρ_b is 0.125/0.125 au, and the frequency is 587.0 cm^{-1} (B3LYP), values that upon complexation with magnesium become 1.630/1.635 Å, 0.167/0.169 au, and 866.2 cm^{-1} (B3LYP), respectively, all indicating a stronger P–O1 bond in the $\text{Mg}-\text{HPO}_4$ complex.

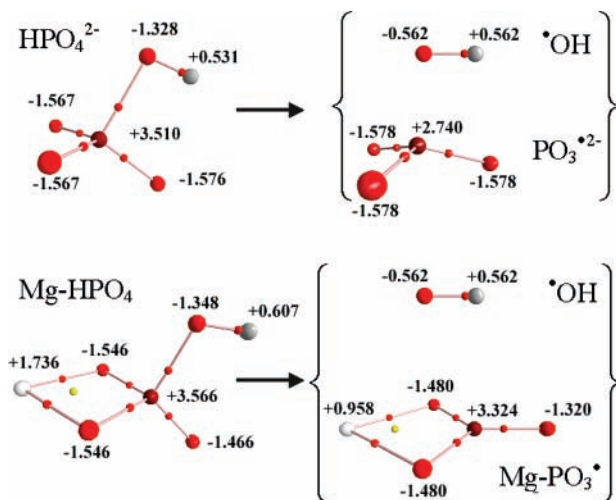
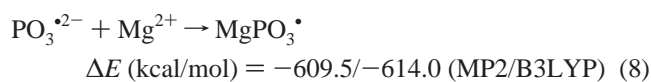
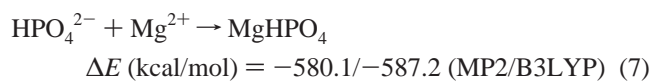


Figure 2. Molecular graphs of the reactants and products of the magnesium-free (top) and Mg^{2+} -mediated homolysis of the P–O1 bond in hydrogen phosphate anion. (Graphs are those of the MP2 calculations; the B3LYP graphs are not displayed as they are topologically identical and otherwise very similar to the MP2 graphs.)

2. Change in Atomic Properties upon the Dissociation of the P–O1 bond in HPO_4^{2-} . Figure 2 provides a display of the molecular graphs⁶ of the species studied in this paper along with the net electrostatic charges. Table 1 compares key atomic properties in the reactants and the products of eqs 5 and 6. The table lists the spin populations $N^{\sigma}(\Omega)$ (defined as the difference between the α - and β -spin populations and assuming nonzero values only for atoms in the open-shell dissociation products), the atomic electron populations $N(\Omega)$, the electrostatic charges $q(\Omega)$, the atomic volumes $\text{vol}(\Omega)$ up to the outer 0.001 au isodensity envelope, and the total atomic energies $E(\Omega)$. The table also lists the change in the atomic energies after the P–O1 bond dissociation, i.e., the atomic contributions to the BDE as defined in eqs 3 and 4 in kcal/mol. Finally, the table lists the changes in the atomic energies of all atoms induced by the complexation with the magnesium cation, changes defined by eqs 7–9,



where the change in an atomic energy due to complexation with magnesium is defined as

$$\Delta E(\Omega)_{\text{Mg}^{2+}} = E(\Omega)_{\text{products}} - E(\Omega)_{\text{reactant}} \quad (9)$$

and where the reactant and products are those in eqs 7 and 8. $\Delta E(\Omega)_{\text{Mg}^{2+}}$ is, thus, the contribution of atom Ω to the binding energy of the magnesium cation to either the intact HPO_4^{2-} (eq 7) or its dissociation product $\text{PO}_3^{\bullet 2-}$ (eq 8).

As can be gleaned from eqs 7 and 8, or equivalently from eqs 5 and 6, complexation with Mg^{2+} favors the dissociation product ($\text{PO}_3^{\bullet 2-}$) over the reactant (HPO_4^{2-}) of eq 5 by 29.5/26.8 kcal/mol. There is thus a thermodynamic advantage in breaking the P–O1 bond in the magnesium complex compared to the free uncomplexed parent molecule.

Table 1 shows that the B3LYP $N^{\sigma}(\Omega)$, $N(\Omega)$, $q(\Omega)$, and $\text{vol}(\Omega)$, are in general good agreement with the MP2 results. Furthermore, the trends in the energy differences are reproduced

(at least qualitatively) in the case of ΔE_{BDE} but the agreement is less satisfactory in the case of $\Delta E(\Omega)_{\text{Mg}^{2+}}$. In the following discussion we will mainly use the (more reliable) MP2 atomic properties and atomic energy contributions and mention the B3LYP values as needed in the case of discrepancies. The definition of atomic energies is reviewed in the Appendix along with an in-depth discussion of the meaning of atomic energies within the KS formulation of density functional theory DFT.

The OH group is negatively charged in the reactants, bearing a net charge of -0.797 e in HPO_4^{2-} , a value slightly reduced by complexation with the magnesium cation to -0.741 e in MgHPO_4 . Naturally, because the BDE is defined for a homolytic cleavage of the P–O1 bond, the OH^\bullet radical in the product of both systems is neutral and identical in both cases. The charge separation in the OH^\bullet radical is $2 \times |0.562|$ e, which is much lower than in the intact reactants, as can be seen from Table 1 (ca. $|-1.328 - 0.531| = 1.859$ e in the case of free HPO_4^{2-} and (ca. $|-1.348 - 0.607| = 1.954$ e in the case of the magnesium complex). The magnesium ion clearly increases the charge separation by almost 0.1 e in the OH group before bond dissociation.

Because the OH^\bullet radical is a common dissociation product regardless of the state of complexation, the effect of complexation on the contribution of this fragment to the BDE stems from the changes induced by the Mg^{2+} cation in the *intact* system. (The contribution from the other dissociation product, obviously, will depend on its state of complexation with magnesium in both the intact and the dissociated state.)

The Mg^{2+} cation destabilizes H in the intact reactant ($\Delta E(\text{H})_{\text{Mg}^{2+}} = 26.4$ kcal/mol) but at the same time stabilizes the oxygen atom of the OH group more significantly ($\Delta E(\text{O1})_{\text{Mg}^{2+}} = -115.3$ kcal/mol). Thus the magnesium cation imparts a net stabilization to the OH fragment in the reactants amounting to 88.9 kcal/mol (the net increase in the OH group contribution to the BDE caused by complexation to Mg^{2+}). In the radical product, the oxygen bears a net electrostatic charge of -0.562 e, but it alone accommodates the unpaired electron, as can be seen from its spin population in Table 1 [$N^{\sigma}(\text{O1}) = 1.0125$ e].

Complexation with magnesium has a more drastic effect on the charge distribution of the dissociation product ($\text{Mg}^\bullet\text{PO}_3$) than on the intact complex ($\text{Mg}^\bullet\text{HPO}_4$), as can be seen from Table 1 and Figure 2. In MgHPO_4 only 0.264 e are gained by the metal neutralizing a small fraction of its (+2 e) positive charge to +1.736 e, the electron gain being mainly at the expense of O2, followed by H, the two atoms at the other extremity of the molecule. This small gain in electronic charge by Mg^{2+} in the intact molecule is to be contrasted with the large gain in charge by the metal in the dissociation product. Thus, in $\text{Mg}^\bullet\text{PO}_3$ the metal gains 1.042 electrons at the expense of the other atoms in this radical, quenching more than half of its original (+2 e) positive charge to +0.958 e.

The effect of the metal in gaining electronic charge at the expense of the phosphorus and the oxygen atoms is much more marked in the dissociation product than in the reactant. In HPO_4^{2-} , the phosphorus is surrounded by four more electronegative oxygen atoms, stripping it from as much as 3.510 e. Complexation of the intact molecule with the magnesium cation (that has the configuration of a Ne atom), results in little changes in the distribution of charge. But when one of the oxygen atoms is missing (in the dissociation product), the electronic charge gained by the phosphorus and the other remaining oxygen atoms (in total, 0.797 e) is readily available to be donated almost completely to the magnesium. As a result, the magnesium in

TABLE 1: Atomic Properties and Their Changes upon Bond Dissociation of Free HPO_4^{2-} and Its Complex with Magnesium (MgHPO_4)

system	atom (Ω)	MP2						B3LYP							
		$N^{\nu}(\Omega)$ (au)	$N(\Omega)$ (au)	$q(\Omega)$ (au)	vol(Ω) (au)	$E(\Omega)$ (au)	$\Delta E(\Omega)_{\text{BDE}}$ (kcal/mol)	$\Delta E(\Omega)_{\text{Mg}}$ (kcal/mol)	$N^{\nu}(\Omega)$ (au)	$N(\Omega)$ (au)	$q(\Omega)$ (au)	vol(Ω) (au)	$E(\Omega)$ (au)	$\Delta E(\Omega)_{\text{BDE}}$ (kcal/mol)	$\Delta E(\Omega)_{\text{Mg}}$ (kcal/mol)
$\text{HPO}_4^{2-} \rightarrow \text{PO}_3^{2-} + \cdot\text{OH}$															
<i>without Mg^{2+}</i>															
reactant (HPO_4^{2-})															
HPO_4^{2-}	H		0.4691	0.5309	24.8	-0.39522			0.4926	0.5074	26.0	-0.41153			
HPO_4^{2-}	O1		9.3280	-1.3280	146.3	-75.57425			9.2886	-1.2886	145.1	-75.60474			
HPO_4^{2-}	P		11.4902	3.5098	32.7	-339.14584			11.5711	3.4289	34.2	-339.97440			
HPO_4^{2-}	O2		9.5764	-1.5764	173.4	-75.62992			9.5543	-1.5543	170.6	-75.66878			
HPO_4^{2-}	O3		9.5674	-1.5674	174.1	-75.64031			9.5456	-1.5456	171.4	-75.68099			
HPO_4^{2-}	O3'		9.5674	-1.5674	174.1	-75.64031			9.5456	-1.5456	171.4	-75.68099			
	sum		49.9986	-1.9986	725.5	-642.02584			49.9978	-1.9978	718.8	-643.02144			
	wfn		50.0000	-2.0000		-642.02569			50.0000	-2.0000		-643.02144			
	diff ^a		0.0014	-0.0014		0.1			0.0022	-0.0022		-0.0			
product ($\text{HO}\cdot$)															
$\text{HO}\cdot$	H	-0.0125	0.4385	0.5615	24.1	-0.38224	8.1	-0.0102	0.4617	0.5383	25.4	-0.39627	9.6		
$\text{HO}\cdot$	O1	1.0125	8.5615	-0.5615	149.0	-75.22200	221.0	1.0102	8.5383	-0.5383	149.1	-75.36687	149.3		
	sum	1.0000	9.0000	-0.0000	173.1	-75.60424		1.0000	9.0000	-0.0000	174.5	-75.76314			
	wfn	1.0000	9.0000	0.0000		-75.60424		1.0000	9.0000	0.0000		-75.76315			
	diff ^a	0.0000	-0.0000	0.0000		-0.0		0.0000	-0.0000	0.0000		-0.0			
product (PO_3^{2-})															
PO_3^{2-}	P	0.5099	12.2600	2.7400	151.9	-339.38062	-147.3	0.4997	12.3755	2.6245	137.4	-340.19902	-141.0		
PO_3^{2-}	O2	0.1615	9.5776	-1.5776	187.9	-75.62171	5.2	0.1627	9.5387	-1.5387	180.5	-75.63093	23.8		
PO_3^{2-}	O3	0.1615	9.5777	-1.5777	187.9	-75.62169	11.7	0.1627	9.5387	-1.5387	180.5	-75.63093	31.4		
PO_3^{2-}	O3'	0.1615	9.5777	-1.5777	187.9	-75.62172	11.7	0.1627	9.5387	-1.5387	180.5	-75.63095	31.4		
	sum	0.9944	40.9931	-1.9931	715.5	-566.24573		0.9877	40.9916	-1.9916	678.8	-567.09183			
	wfn	1.0000	41.0000	-2.0000		-566.24479		1.0000	41.0000	-2.0000		-567.09286			
	diff ^a	0.0056	0.0069	-0.0069		0.6		0.0123	0.0084	-0.0084		-0.7			
sum $\Delta E(\Omega)$							110.4								104.5
$\text{MgHPO}_4 \rightarrow \text{MgPO}_3\cdot + \cdot\text{OH}$															
<i>with Mg^{2+}</i>															
reactant ($\text{Mg}-\text{HPO}_4$)															
$\text{Mg}-\text{HPO}_4$	H		0.3931	0.6069	21.1	-0.35312	26.4		0.4101	0.5899	21.8	-0.36793	27.4		
$\text{Mg}-\text{HPO}_4$	O1		9.3475	-1.3475	130.5	-75.75797	-115.3		9.3048	-1.3048	128.9	-75.77738	-108.3		
$\text{Mg}-\text{HPO}_4$	P		11.4339	3.5661	30.3	-339.23147	-53.7		11.5157	3.4843	31.9	-339.98650	-7.6		
$\text{Mg}-\text{HPO}_4$	O2		9.4660	-1.4660	154.6	-75.76994	-87.9		9.4382	-1.4382	152.1	-75.79381	-78.5		
$\text{Mg}-\text{HPO}_4$	O3		9.5457	-1.5457	152.1	-75.70812	-42.5		9.5060	-1.5060	148.4	-75.72979	-30.6		
$\text{Mg}-\text{HPO}_4$	O3'		9.5457	-1.5457	152.1	-75.70812	-42.5		9.5060	-1.5060	148.4	-75.72979	-30.6		
$\text{Mg}-\text{HPO}_4$	Mg		10.2639	1.7361	57.6	-199.37107			10.3149	1.6851	66.2	-199.81386			
	sum		59.9959	0.0041	698.3	-841.89980	-315.6		59.9957	0.0043	697.6	-843.19906	-228.3		
	wfn		60.0000	0.0000		-841.89989			60.0000	0.0000		-843.19904			
	diff ^a		0.0041	-0.0041		-0.1			0.0043	-0.0043		0.0			
product ($\text{HO}\cdot$)															
$\text{HO}\cdot$	H	-0.0125	0.4385	0.5615	24.1	-0.38224	-18.3	-0.0102	0.4617	0.5383	25.4	-0.39627	-17.8		
$\text{HO}\cdot$	O1	1.0125	8.5615	-0.5615	149.0	-75.22200	336.3	1.0102	8.5383	-0.5383	149.1	-75.36687	257.6		
	sum	1.0000	9.0000	-0.0000	173.1	-75.60424		1.0000	9.0000	-0.0000	174.5	-75.76314			
	wfn	1.0000	9.0000	0.0000		-75.60424		1.0000	9.0000	0.0000		-75.76315			
	diff ^a	0.0000	-0.0000	0.0000		-0.0		0.0000	-0.0000	0.0000		-0.0			
product ($\text{MgPO}_3\cdot$)															
$\text{MgPO}_3\cdot$	P	0.0075	11.6761	3.3239	52.0	-339.50402	-171.0	-77.4	0.0150	11.7205	3.2795	53.4	-340.17580	-118.8	14.6
$\text{MgPO}_3\cdot$	O2	0.0060	9.3200	-1.3200	149.8	-75.72012	31.3	-61.8	0.0130	9.3146	-1.3146	148.3	-75.74323	31.7	-70.5
$\text{MgPO}_3\cdot$	O3	0.0436	9.4803	-1.4803	150.7	-75.74665	-24.2	-78.4	0.0531	9.4649	-1.4649	148.6	-75.76626	-22.9	-84.9
$\text{MgPO}_3\cdot$	O3'	0.0436	9.4803	-1.4803	150.6	-75.74665	-24.2	-78.4	0.0531	9.4649	-1.4649	148.6	-75.76626	-22.9	-84.9
$\text{MgPO}_3\cdot$	Mg	0.8991	11.0422	0.9578	218.6	-199.44859	-48.6		0.8654	11.0328	0.9672	209.5	-199.86154	-29.9	
	sum	0.9998	50.9990	0.0010	721.7	-766.16603		-296.0	0.9996	50.9977	0.0023	708.3	-767.31309	-225.7	
	wfn	1.0000	51.0000	0.0000		-766.16594			1.0000	51.0000	0.0000		-767.31314		
	diff ^a	0.0002	0.0010	-0.0010		0.1		0.0004	0.0023	-0.0023		-0.0			
sum $\Delta E(\Omega)$							81.3								77.1

^a Differences between molecular values and the sum of atomic values. All entries in au except differences in energy given in kcal/mol.

$\text{MgPO}_3\cdot$ bears $q(\Omega) = +0.958$ e; i.e., it has gained 0.778 e after the dissociation of the P–O1 bond.

Accompanying these population changes is a dramatic magnesium-induced rearrangement of the spin density and population in the radical dissociation product, as can be seen from Table 1 and Figure 3. From Figure 3, the $\text{PO}_3\cdot$ doublet is slightly pyramidalized (the height of the phosphorus atom over the plane of the three oxygen atom is 0.2074 Å). The spin density accumulates primarily in the basin of the phosphorus atom on the convex side of the radical, the spin population of this atom being 0.510 e, whereas the oxygen atoms share the

rest of the spin population. The complexation with the magnesium cation results in a perfectly flat structure.

The volume of each atom changes appreciably after the dissociation of the P–O1 bond in both the magnesium-free system and in the magnesium complex. The volume of the P atom increases dramatically from 32.7 au in the magnesium-free reactant to 151.9 au in its radical dissociation product (see Table 1). This large volume increase is attributed to the localization of unpaired spin population into the atomic basin of the phosphorus (the spin population of this atom is 0.5099 e). In the magnesium complex, Table 1 also shows an

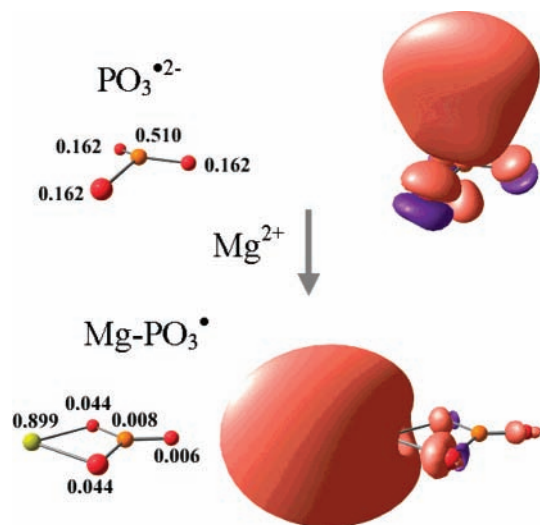


Figure 3. Spin populations (left) and 0.001 au spin isodensity envelopes [orange envelopes for positive values (excess α -spin density) and violet envelopes for negative spin density (excess β -spin density)].

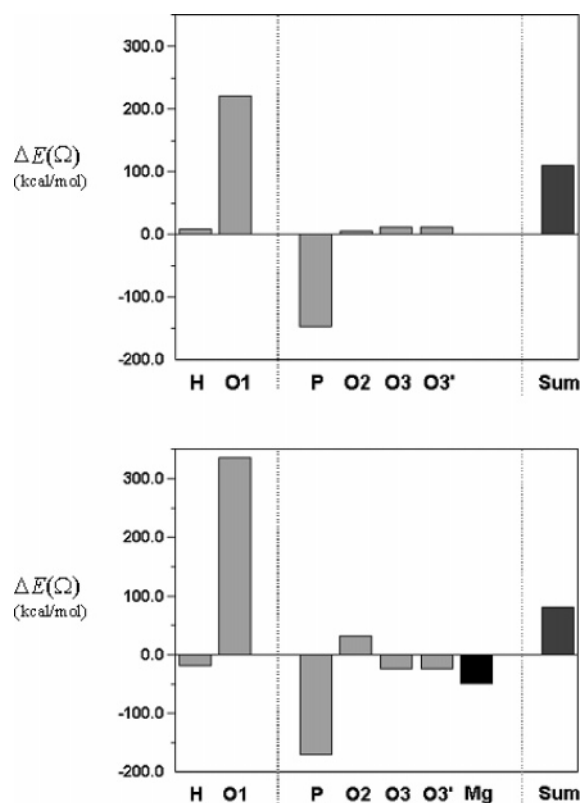


Figure 4. Display of the *change* in the energy of each atom [$\Delta E(\Omega)$ in kcal/mol] in the magnesium-free molecule (top) and in the magnesium complex (bottom) upon dissociation of the P–O1 bond calculated at the (U)MP2/6-311++G(d,p)//(U)MP2/6-311++G(d,p) level of theory. The height of the bar depicts the magnitude of the atomic contributions of each atom to the electronic vibrationless bond dissociation energy BDE. The sign of the contribution is positive if the atom is destabilized upon bond breaking and negative if the atom is stabilized upon breaking. The contribution of each atom is shaded in light gray, the contribution of the magnesium cation in black, and the sum of all contributions (equivalent to the BDE is in dark gray). (Compare with Figure 5.)

increase in the volume of the phosphorus after the breaking of the bond, but this increase, though still significant (from 30.3 au to 52.0 au), is much less than in the magnesium-free case. Breaking the P–O1 bond results in a substantial increase in

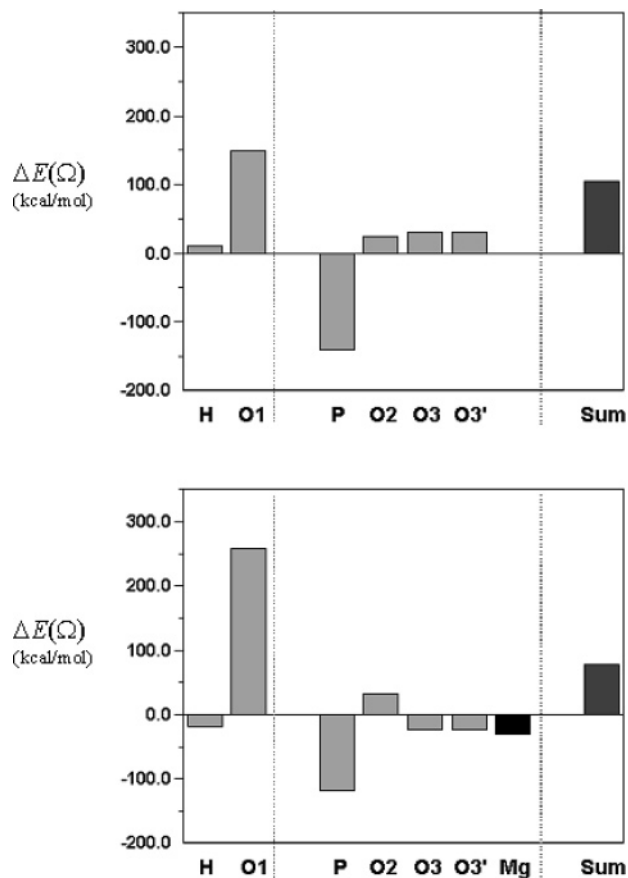


Figure 5. Bar chart showing the *change* in the energy of each atom [$\Delta E(\Omega)$ in kcal/mol] in the magnesium-free molecule (top) and in the magnesium complex (bottom) upon dissociation of the P–O1 bond, calculated at the (U)B3LYP/6-311++G(d,p)//(U)B3LYP/6-311++G(d,p) level of theory. (See Figure 4 and its caption for comparison and further explanation, respectively.)

the volume of the magnesium cation (from 57.2 au to 218.6 au) as its basin gains both net total electron and spin populations (Table 1).

In both the free and the complexed reactants, the dissociation of the P–O1 bond entails a large stabilization of the phosphorus atom that gains electron population as a result of the removal of one of its (more electronegative) oxygen ligands [$\Delta N(\text{P}) = 0.770$ e in the magnesium-free case and 0.242 e in the case of the metal complex]. The phosphorus atom in the case of the metal complex is 171.0 kcal/mol more stable in the dissociation product when compared with the reactant. This value decreases to only 147.3 kcal/mol in the metal-free case. Furthermore, in the absence of the magnesium cation, the atomic contributions of the remaining atoms, the three oxygen atoms, are all positive (5.2, 11.7, and 11.7 kcal/mol, totalling 28.6 kcal/mol); i.e., these atoms are more stable in the intact molecule (Table 1). The presence of the Mg^{2+} ion reverses the sign and roughly doubles the magnitudes of the contributions of O3 and O3' while significantly increasing the positive contribution of O2; the net result is a stabilization of the three oxygen atoms in the dissociation product of the complex by 17.1 kcal/mol ($31.3 - 24.2 - 24.2 = -17.1$ kcal/mol). In the magnesium-free case, the combined contributions of these three oxygen atoms is a net destabilization of the dissociation product by 28.6 kcal/mol ($5.2 + 11.7 + 11.7 = +28.6$ kcal/mol). Finally, the magnesium atom itself has a negative contribution of -48.6 kcal/mol, i.e., favors the bond dissociation. The atomic contributions to the BDE are represented in Figure 4 (MP2 calculations) and Figure

TABLE 2: Bond Properties and Their Changes upon Bond Dissociation of Free HPO_4^{2-} and Its Complex with Magnesium (MgHPO_4)^a

system bond	MP2								B3LYP							
	BL	ρ_b	$\nabla^2\rho_b$	ϵ	K_b	G_b	V_b	H_b	BL	ρ_b	$\nabla^2\rho_b$	ϵ	K_b	G_b	V_b	H_b
without Mg^{2+}																
HPO_4^{2-} H–O1	0.961	0.362	-2.421	0.018	0.698	0.093	-0.790	-0.698	0.962	0.366	-2.403	0.019	0.685	0.085	-0.770	-0.685
HPO_4^{2-} P–O1	1.772	0.125	0.224	0.035	0.093	0.149	-0.242	-0.093	1.787	0.125	0.151	0.038	0.094	0.132	-0.226	-0.094
HPO_4^{2-} P–O2	1.553	0.199	1.005	0.025	0.150	0.401	-0.550	-0.150	1.556	0.201	0.934	0.028	0.153	0.387	-0.540	-0.153
HPO_4^{2-} O3/O3'	1.537	0.205	1.093	0.031	0.154	0.427	-0.580	-0.154	1.540	0.207	1.025	0.035	0.158	0.414	-0.571	-0.158
PO_3^{2-} P–O2/O3/O3'	1.528	0.204	1.157	0.124	0.149	0.438	-0.587	-0.149	1.545	0.210	1.175	0.033	0.154	0.447	-0.601	-0.154
HO^{\bullet} O–H	0.969	0.362	-2.516	0.042	0.707	0.078	-0.785	-0.707	0.976	0.358	-2.409	0.044	0.672	0.070	-0.742	-0.672
with Mg^{2+}																
Mg-HPO_4 H–O1	0.962	0.355	-2.480	0.016	0.699	0.079	-0.778	-0.699	0.964	0.358	-2.409	0.044	0.672	0.070	-0.742	-0.672
Mg-HPO_4 P–O1	1.630	0.167	0.666	0.061	0.121	0.287	-0.408	-0.121	1.635	0.169	0.595	0.069	0.124	0.273	-0.397	-0.124
Mg-HPO_4 P–O2	1.481	0.231	1.491	0.017	0.174	0.547	-0.721	-0.174	1.482	0.233	1.421	0.017	0.178	0.533	-0.711	-0.178
Mg-HPO_4 P–O3/O3'	1.614	0.176	0.714	0.019	0.132	0.310	-0.442	-0.132	1.619	0.178	0.643	0.013	0.135	0.296	-0.432	-0.135
Mg-HPO_4 Mg–O3/O3'	1.886	0.062	0.507	0.033	-0.012	0.115	-0.102	0.012	1.879	0.064	0.510	0.036	-0.012	0.115	-0.103	0.012
MgPO_3^{\bullet} P–O2	1.465	0.233	1.609	0.137	0.171	0.573	-0.744	-0.171	1.464	0.237	1.562	0.132	0.177	0.567	-0.744	-0.177
MgPO_3^{\bullet} P–O3/O3'	1.526	0.208	1.182	0.153	0.153	0.449	-0.602	-0.153	1.527	0.211	1.124	0.156	0.158	0.439	-0.597	-0.158
MgPO_3^{\bullet} Mg–O3/O3'	2.113	0.035	0.230	0.072	-0.007	0.051	-0.044	0.007	2.108	0.036	0.229	0.058	-0.007	0.051	-0.044	0.007

^a All entries in au except bond lengths (BL) listed in Å.

5 (B3LYP calculations). The sum of the atomic contributions to the BDE due to atoms in the PO_3^{2-} is -118.7 kcal/mol in the metal-free case, a value that reaches -236.7 kcal/mol in MgPO_3^{\bullet} .

The Mg^{2+} destabilizes H in the intact reactant ($\Delta E(\text{H})_{\text{Mg}^{2+}} = 26.4$ kcal/mol) but at the same time stabilizes the O1 atom more significantly ($\Delta E(\text{O1})_{\text{Mg}^{2+}} = -115.3$ kcal/mol). Thus the magnesium cation imparts a net stabilization to the OH fragment in the reactants amounting to 88.9 kcal/mol (the net increase in the OH group contribution to the BDE caused by complexation to Mg^{2+}).

Figures 4 and 5 display the atomic contributions to the BDE in the presence and absence of the magnesium cation at the MP2 and the B3LYP levels of theory, respectively. In these figures, a negative contribution favors bond dissociation and a positive contribution favors the intact molecule. By juxtaposing the plot in the absence (top) and presence (bottom) of the Mg^{2+} , the effect of the cation can be visualized. The complexation with magnesium disturbs the size and sign of the contributions of the rest of the atoms in the system with the net result of reducing the sum (the BDE), i.e., favoring bond dissociation.

Summing up, the contribution to the BDE of the OH fragment is unfavorable (positive) to bond dissociation in both cases ($+229.1$ and $+318.0$ kcal/mol for the magnesium-free and the magnesium-complex cases, respectively), being more unfavorable in the case of the magnesium complex with a net difference of 88.9 kcal/mol. The contribution of the phosphorus-containing fragment is favorable in both cases (-118.7 and -236.7 kcal/mol for the magnesium-free and the magnesium-complex cases, respectively), being more favorable in the case of the magnesium complex with a net 118.0 kcal/mol. Magnesium, thus, facilitates the P–O1 bond dissociation by 29.1 kcal/mol when compared to the metal-free reaction, accounting for the difference between $\Delta E_{\text{electronic}}$ in eqs 5 and 6.

3. Change in Bond Properties upon the Dissociation of the P–O1 bond and upon Complexation with Magnesium. Table 2 lists some bond properties of the free and complexed reactants and products. The data in the table show very good agreement not only in trends but also in individual numerical values obtained at the MP2 and B3LYP levels of theory.

Table 2 also reveals that the complexation with magnesium results in the lengthening of the H–O1 and P–O3(or O3') bonds but has the opposite effects on the P–O1 and the P–O2 bonds. The significant shortening of the latter two bonds is accompanied by a significant increase in the electron density at the BCP (ρ_b),

an increase in $\nabla^2\rho_b$, and a significant increase in the magnitude of the (negative) total energy density evaluated at the BCP (H_b). These trends are consistent with a “strengthening” of these two bonds in the magnesium complex compared with the metal-free case. This observation is corroborated with a substantial increase in the vibrational stretching frequency of the P–O1 bond upon complexation with the Mg^{2+} form 587.0 cm^{-1} in the free anion to 866.2 cm^{-1} in the complex (unscaled frequencies from the B3LYP calculations). In contrast, thermodynamically, the magnesium reduces the BDE and therefore “weakens” the P–O1 bond rather than strengthening it. This is an example where the relative strength of a given chemical bond cannot be inferred from descriptors such as bond lengths in the intact system, as is often the case for example for C–C bonds.³¹ Politzer and Habibollahzadeh state that

“for a given type of bond in different molecular environments, an inverse relationship is normally assumed to exist between its force constant k and length R ... both k and R are commonly taken to be measures of bond strength, D : $D \sim k$ and $D \sim 1/R$.”³²

in a paper where they describe another type of deviation from this rule, namely an anomalous variation in bond length with the BDE (but not k).³² In the present work, k and R change consistently with one another but inconsistently with D .

The character of the magnesium–oxygen bonds is of particular interest. This bond exhibits characteristics of a closed-shell interaction in both the intact reactant (MgHPO_4) and its dissociation doublet radical product (MgPO_3^{\bullet}). Thus, in these two cases, the bond exhibits a small ρ_b along with a positive H_b of small magnitude, both markers of a closed-shell bonding interaction.

Upon breaking the P–O1 bond, the closed-shell bonding interaction between the magnesium and the two oxygen atoms become 0.227 Å longer with a concomitant marked reduction in ρ_b (from 0.062 au to only 0.035 au). This lengthening of the Mg–O bonds after the breaking of the P–O1 bond reflect the larger size of the magnesium ion that jumps from 57.6 au to 218.6 au.

Conclusions

The complexation of HPO_4^{2-} with magnesium results in the shortening of the P–O1 bond, an increase in its stretching vibrational frequency, a higher electron density at the BCP, and a more negative total (and potential) energy density at the bond

critical point. This apparent strengthening of the P–O1 bond (if one relies on the above-mentioned oft-used bond strength indicators) is accompanied by a thermodynamic weakening of this bond. In other words, the homolytic cleavage of the P–O1 bond in the magnesium complex requires *less* energy than in the magnesium-free case. This is mainly due to a preferential binding of the magnesium to the phosphorus-containing radical dissociation product compared to the binding of this metal to the intact reactant. We conclude, thus, that an individual bond may be strengthened by complex formation but the dissociation is globally more favorable because of other more dominant driving forces.

The inverse correlation between bond strength descriptors in the intact molecule and BDE do not rule out a correlation between bond strength and the barrier to dissociation, even though the barrier and the energy of reaction are not infrequently correlated, as predicted from Hammond's postulate.³³ We are currently investigating the role of magnesium on the dissociation barrier of phosphorylated compounds when coupled with hydrolysis.

Appendix A: Atomic Energies for *ab Initio* Methods

For a molecule described by an exact stationary state Born–Oppenheimer wavefunction Ψ and at an equilibrium geometry, any atom Ω in the molecule satisfies the following virial theorem:⁶

$$2T(\Omega) + V_{\text{ne}}(\Omega) + V_{\text{ee}}(\Omega) + V_{\text{nn}}(\Omega) = 2T(\Omega) + V(\Omega) = 0 \quad (\text{A1})$$

where $T(\Omega)$ is the electronic kinetic energy of the atom and $V_{\text{ne}}(\Omega)$, $V_{\text{ee}}(\Omega)$, and $V_{\text{nn}}(\Omega)$ are the nuclear–electron attraction, electron–electron repulsion, and nuclear–nuclear repulsion potential energy contributions from the atom. Although $T(\Omega)$, $V_{\text{ne}}(\Omega)$, and $V_{\text{ee}}(\Omega)$ have rather straightforward expressions similar to those for the molecule as a whole, the nuclear repulsion contribution $V_{\text{nn}}(\Omega)$ is a less obvious origin-independent (for exact wavefunctions) sum of three origin-dependent terms (see section 6.3.4 of Bader's book⁶ for explicit expressions for these terms):

$$V_{\text{nn}}(\Omega) = \sum_{A=1}^{n_{\text{atoms}}} \mathbf{R}_A \cdot \mathbf{F}_A(\Omega) + V(\Omega, \Omega') + \mathcal{V}'_{\zeta}(\Omega) \quad (\text{A2})$$

The contributions $V_{\text{nn}}(\Omega)$ are additive to give the molecular V_{nn} because of the molecular Hellmann–Feynman electrostatic theorem and because the terms $V(\Omega, \Omega')$ sum to zero for the molecule, as do the $\mathcal{V}'_{\zeta}(\Omega)$ terms.

Equation A1 is unique to atoms in molecules (and groups of atoms in molecules) both in its variational derivation and because only for atoms in molecules is the kinetic energy always well-defined.⁶

Similar to the molecular energy E , an atomic energy $E(\Omega)$ is defined as the sum of kinetic and potential contributions as follows:⁶

$$E(\Omega) = T(\Omega) + V_{\text{ne}}(\Omega) + V_{\text{ee}}(\Omega) + V_{\text{nn}}(\Omega) = T(\Omega) + V(\Omega) \quad (\text{A3})$$

Combining eqs A1 and A3, one obtains the following simple relationship between $E(\Omega)$ and $T(\Omega)$ and between $E(\Omega)$ and $V(\Omega)$:

$$E(\Omega) = -T(\Omega) = \frac{1}{2}V(\Omega) \quad (\text{A4})$$

Equations A1, A3, and A4 are applicable not only to atoms in molecules but also to groups of atoms in molecules and, of course, the molecule as a whole. When referring to energetic terms for the molecule as a whole, we omit the “(Ω)” suffix.

Being able to express the total atomic energy $E(\Omega)$ in terms of the atomic kinetic energy $T(\Omega)$ drastically simplifies its calculation and, in some ways, its interpretation.

For a typical *approximate* wavefunction Ψ_{approx} , however, the atomic and molecular virial theorems will *not* be exactly satisfied. The consequence of this is that calculating atomic energies using eq A4 will *not* result in energy additivity, i.e.,

$$\sum_{\Omega=1}^{n_{\text{atoms}}} [-T(\Omega)] = -T \neq E \quad (\text{for approximate, noncoordinate-scaled wavefunctions}) \quad (\text{A5})$$

Another consequence of typical approximate wavefunctions is that the atomic energy contribution $V_{\text{nn}}(\Omega)$ defined in eq A2 will be origin-dependent,³⁴ thus making the direct evaluation of atomic energies $E(\Omega)$ using eq A3 ambiguous. In addition, the $V_{\text{nn}}(\Omega)$ contributions will *not* be additive to give the molecular value V_{nn} unless the wavefunction satisfies the molecular Hellmann–Feynman electrostatic theorem for all nuclei,³⁴ a stringent requirement not satisfied by typical approximate wavefunctions. The direct evaluation of atomic energies using eq A3 thus does *not* guarantee energy additivity for typical approximate wavefunctions. Even in cases where the Hellmann–Feynman electrostatic theorem is satisfied for all nuclei and energy additivity is obtained using eq A3, each atomic energy $E(\Omega)$ will still be origin-dependent due to the $V_{\text{nn}}(\Omega)$ term, in addition to being difficult and costly to calculate. The origin-independence of the atomic kinetic energy is another good reason for using eq A4 to calculate the atomic energy, assuming the problem of energy additivity expressed by eq A5 is addressed.

Energy additivity for atomic energies defined by atomic kinetic energies using eq A4 *can* be obtained if the coordinates of the wavefunction are scaled using the following factor ζ .^{35,36}

$$\zeta = -\frac{1}{2} \frac{V}{T} = -\frac{1}{2} \left(\frac{E}{T} - 1 \right) \quad (\text{A6})$$

It proves enlightening to express ζ in terms of 1 plus a (small) correction term ϵ , which vanishes for wavefunctions satisfying the molecular virial theorem, as follows:

$$\zeta = \frac{1}{2} - \frac{1}{2} \frac{E}{T} = 1 - \frac{1}{2} \frac{E}{T} - \frac{1}{2} = 1 + \epsilon \quad (\text{A7})$$

where

$$\epsilon = -\frac{1}{2} \frac{E}{T} - \frac{1}{2} = -\frac{1}{2} \frac{V}{T} - 1 \quad (\text{A8})$$

Using a (renormalized) wavefunction Ψ_{ζ} , whose coordinates have been scaled by ζ , the molecular kinetic energy T_{ζ} , potential energy V_{ζ} , and total energy E_{ζ} are given by

$$T_{\zeta} = \zeta^2 T = T + 2\epsilon T + \epsilon^2 T = \frac{(E - T)^2}{4T} \quad (\text{A9})$$

$$V_\zeta = \zeta V = V + \epsilon V = -\frac{(E - T)^2}{2T} \quad (\text{A10})$$

and

$$\begin{aligned} E_\zeta &= T_\zeta + V_\zeta = T + 2\epsilon T + \epsilon^2 T + V + \epsilon V \\ &= T + 2\epsilon T + \epsilon^2 T - \epsilon(1 + \epsilon)2T \\ &= T + 2T\epsilon + T\epsilon^2 - 2T\epsilon - 2T\epsilon^2 \\ &= T - T\epsilon^2 \\ &= -\frac{(E - T)^2}{4T} \\ &= 2V_\zeta = -T_\zeta \end{aligned} \quad (\text{A11})$$

These equations show that the energies T_ζ , V_ζ , and E_ζ from the coordinate scaled wavefunction Ψ_ζ satisfy the molecular virial theorem and, equally important, that the energy E_ζ is quadratic in the (small) correction ϵ whereas both T_ζ and V_ζ are linear in the (small) correction ϵ . In other words, coordinate scaling of the wavefunction to satisfy the molecular virial theorem will change the kinetic and potential energy components T and V much more than the total energy E .

Unfortunately, such a coordinate scaling of the wavefunction will also lead to forces on the nuclei as well as make the energy nonstationary with respect to the variational parameters in the wavefunction.^{35,36} In addition, some atomic and molecular properties calculated using the unscaled wavefunction Ψ will be inconsistent with the energies calculated from the scaled wavefunction. Thus, ideally, coordinate scaling of the wavefunction to satisfy the molecular virial theorem should be done *self-consistently* with geometry optimization and the wavefunction determination, leading to a valid variational and/or perturbational wavefunction, satisfaction of the molecular virial theorem, a true equilibrium geometry, and a consistent set of atomic and molecular properties.

It should be noted that coordinate scaling of the wavefunction to satisfy the molecular virial theorem does *not* guarantee satisfaction of the individual atomic virial theorems.³⁴

In many cases, a computationally simpler and commonly used⁶ procedure for obtaining energy additivity for atomic energies calculated using eq A4, when the wavefunction does not satisfy the molecular virial theorem, is simply to scale the atomic kinetic energies $T(\Omega)$ by E/T . This simpler procedure does *not* correspond to a coordinate scaling of the wavefunction but is the procedure employed in this paper for the ab initio MP2 energies:

$$E(\Omega) = \frac{E}{T} T(\Omega) \quad (\text{A12})$$

Equation A12 is a valid approximation to a coordinate scaling result if the change in total molecular energy E brought about by coordinate scaling is relatively small *and* if the change in each atomic kinetic energy brought about by coordinate scaling is directly proportional (by the same factor for all atoms, and hence for the molecule) to the corresponding unscaled atomic kinetic energy.

Appendix B: Atomic Energies for Kohn–Sham Density Functional Theory Methods

For Kohn–Sham DFT (KSDFT) methods,³⁷ such as the B3LYP^{38,39} method employed in this paper, the definition and

calculation of atomic energies is less clear than for ab initio, i.e., Hamiltonian-based, wavefunction methods such as Hartree–Fock or MP2. However, if one views KSDFT theory as a semiempirical variant of Hartree–Fock theory, then one can follow a procedure similar to that given in Appendix A, albeit with a somewhat different interpretation. The atomic virial theorem corresponding to eq A1 for KSDFT methods is⁴⁰

$$2T_s(\Omega) + V_{\text{ne}}(\Omega) + V_{\text{ee,H}}(\Omega) + V_{\text{nn}}(\Omega) + E_{\text{xc}}(\Omega) + T_c(\Omega) = 0 \quad (\text{B1})$$

where $T_s(\Omega)$ is the so-called “noninteracting” kinetic energy of atom Ω , $V_{\text{ne}}(\Omega)$ is the nuclear–electron attraction energy contribution from atom Ω , $V_{\text{ee,H}}(\Omega)$ is the “Hartree” (i.e., electrostatic) contribution of atom Ω to the electron–electron potential energy, and $V_{\text{nn}}(\Omega)$ has the same expression as given in eq A2. The atomic “exchange–correlation” energy $E_{\text{xc}}(\Omega)$ and correlation kinetic energy $T_c(\Omega)$ are related to the virial of the exchange–correlation potential $v_{\text{xc}}(\mathbf{r})$ as follows:

$$E_{\text{xc}}(\Omega) + T_c(\Omega) = V_{\text{xc}}(\Omega) + 2T_c(\Omega) = -\int_{\Omega} d\mathbf{r} \rho(\mathbf{r}) \mathbf{r} \cdot \nabla v_{\text{xc}}(\mathbf{r}) \quad (\text{B2})$$

This equation is a generalization to atoms in molecules of the Levy and Perdew result.⁴¹

The definition of $v_{\text{xc}}(\mathbf{r})$ depends, of course, on the particular KSDFT method used. Also, it is very important to realize that the atomic exchange–correlation energy, $E_{\text{xc}}(\Omega)$, consists of a kinetic contribution $T_c(\Omega)$ and a purely potential contribution $V_{\text{xc}}(\Omega)$.

If one defines the atomic energy $E(\Omega)$ in a KSDFT method as

$$E(\Omega) = T_s(\Omega) + V_{\text{ne}}(\Omega) + V_{\text{ee,H}}(\Omega) + V_{\text{nn}}(\Omega) + E_{\text{xc}}(\Omega) \quad (\text{B3})$$

then one gets energy additivity, assuming that the KSDFT method’s “wavefunction” satisfies the Hellmann–Feynman electrostatic theorem for all nuclei and thus that the $V_{\text{nn}}(\Omega)$ are additive to give V_{nn} at equilibrium geometries.

Combining eqs B1 and B3, one gets the following relationship:

$$E(\Omega) = -[T_s(\Omega) + T_c(\Omega)] = -T(\Omega) \quad (\text{B4})$$

As for ab initio methods, this relationship will not be satisfied either at the atomic or at molecular levels by typical approximate KSDFT “wavefunctions”. However, just as for ab initio methods, coordinate scaling of the KSDFT “wavefunction” can be done to satisfy $E = -T$ for the molecule and additivity of the atomic energies calculated using eq B4.

The KSDFT relationship between the atomic energy and total atomic kinetic energy is the same as for ab initio methods, but the atomic kinetic energy now consists of two contributions, the readily accessible “noninteracting” kinetic energy, whose expression is the same as for Hartree–Fock, and the “correlation” kinetic energy, which can in principle be determined from eq B4, if $E_{\text{xc}}(\Omega)$ is determined separately.

The molecular correlation kinetic energy T_c is believed to be on the order of the correlation energy itself, $T_c \sim -E_c$,⁴² and therefore much smaller than the molecular “noninteracting” kinetic energy T_s . If one simply ignores T_c and $T_c(\Omega)$, then one may calculate an atomic energy from $T_s(\Omega)$ by simply scaling $T_s(\Omega)$ by the factor E/T_s :

$$E(\Omega) = \frac{E}{T_s} T_s(\Omega) \quad (\text{B5})$$

This is the definition of the B3LYP atomic energies employed here, and it is similar to the definition used for the ab initio MP2 atomic energies used here, eq A12. The validity of this expression, compared to using the full kinetic energies T and $T(\Omega)$, either requires that $T_c \ll T_s$ and $T_c(\Omega) \ll T_s(\Omega)$ or requires that $T_c = aT_s$ and $T_c(\Omega) = aT_s(\Omega)$, as shown here

$$\frac{1}{(T_s + T_c)} = \frac{1}{T_s} - \frac{T_c}{(T_s + T_c)^2} + \frac{T_c^2}{(T_s + T_c)^3} + \dots \quad (\text{B6a})$$

$$\begin{aligned} E(\Omega) &= \frac{E}{T} T(\Omega) = \left[\frac{E}{(T_s + T_c)} \right] [T_s(\Omega) + T_c(\Omega)] \\ &= \left[\frac{T_s(\Omega)}{T_s} - \frac{T_s(\Omega)T_c}{(T_s + T_c)^2} + \frac{T_s(\Omega)T_c^2}{(T_s + T_c)^3} + \dots \right] + \\ &\quad \left[\frac{T_c(\Omega)}{T_s} - \frac{T_c(\Omega)T_c}{(T_s + T_c)^2} + \frac{T_c(\Omega)T_c^2}{(T_s + T_c)^3} + \dots \right] \\ &= \frac{E}{T_s} T_s(\Omega) \quad [\text{if } T_c \ll T_s \text{ and } T_c(\Omega) \ll T_s(\Omega)] \quad (\text{B6b}) \end{aligned}$$

If

$$T_c = aT_s \quad T_c(\Omega) = aT_s(\Omega) \quad (\text{B7a})$$

Then

$$\begin{aligned} E(\Omega) &= \frac{E}{T} T(\Omega) = \left[\frac{E}{(T_s + aT_s)} \right] [T_s(\Omega) + aT_s(\Omega)] \\ &= \left[\frac{E}{(1 + a)T_s} \right] [1 + a]T_s(\Omega) = \frac{E}{T_s} T_s(\Omega) \quad (\text{B7b}) \end{aligned}$$

Acknowledgment. We acknowledge the Natural Sciences and Engineering Research Council of Canada (NSERC) and Mount Saint Vincent University for funding. C.F.M. thanks Professor Claude Lecomte [Laboratoire de Cristallographie et Modélisation des Matériaux Minéraux et Biologiques (LCM3B), Université Henri Poincaré, and CNRS, Nancy, France] for an invited professorship during which this paper was finalized.

References and Notes

- Pauling, L. *The Nature of the Chemical Bond*, 3rd ed.; Cornell University Press: Ithaca, NY, 1960.
- Szwarc, M.; Evans, M. G. *J. Chem. Phys.* **1950**, *18*, 618–622.
- Gaydon, A. G. *Dissociation Energies and Spectra of Diatomic Molecules*, 3rd ed.; Chapman and Hall, Ltd.: London, 1968.
- Marks, T. J. *Bonding Energetics in Organometallic Compounds*; American Chemical Society: Washington, DC, 1990.
- Luo, Y.-R. *Handbook of Bond Dissociation Energies in Organic Compounds*; CRC Press: New York, 2003.
- Bader, R. F. W. *Atoms in Molecules: A Quantum Theory*; Oxford University Press: Oxford, U.K., 1990.
- Popelier, P. L. A. *Atoms in Molecules: An Introduction*; Prentice Hall: London, 2000.
- Matta, C. F.; Boyd, R., Eds. *The Quantum Theory of Atoms in Molecules: From Solid State to DNA and Drug Design*; Wiley-VCH: Weinheim, 2007.
- Matta, C. F.; Castillo, N.; Boyd, R. *J. Chem. Phys.* **2006**, *125*, 204103_1–204103_13.
- Gomez-Tagle, P.; Vargas-Zúñiga, I.; Taran, O.; Yatsimirsky, A. K. *J. Org. Chem.* **2006**, *71*, 9713–9722.
- Larson, A. C. *Acta Crystallogr. B* **1978**, *34*, 3601–3604.
- Wang, P.; Izatt, R. M.; Oscarson, J. L.; Gillespie, S. E. *J. Phys. Chem.* **1996**, *100*, 9556–9560.
- Kennard, O.; Isaacs, N. W.; Motherwell, W. D. S.; Coppola, J. C.; Wampler, D. L.; Larson, A. C.; Watson, D. G. *Proc. R. Soc. London A* **1971**, *325*, 401–436.
- Saint-Martin, H.; Ruiz-Vicent, L. E.; Ramirez-Solis, A.; Ortega-Blake, I. *J. Am. Chem. Soc.* **1996**, *118*, 12167–12173.
- Franzini, E.; Fantucci, P.; De Gioia, L. *J. Mol. Catal. A: Chem.* **2003**, *204–205*, 409–417.
- Yoshikawa, K.; Shinohara, Y.; Terada, H.; Kato, S. *Biophys. Chem.* **1987**, *27*, 251–254.
- Admiraal, S. J.; Herschlag, D. *Chem. Biol.* **1995**, *2*, 729–739.
- Tulub, A. A. *Phys. Chem. Chem. Phys.* **2006**, *8*, 2187–2192.
- Williams, N. H. *Biochem. Biophys. Acta* **2004**, *1697*, 279–287.
- Tajima, M.; Honda, M. *J. Mol. Struct. (THEOCHEM)* **1991**, *228*, 201–208.
- Banks, B. E. C.; Vernon, C. A. *J. Theor. Biol.* **1970**, *29*, 301–326.
- McClare, C. W. F. *J. Theor. Biol.* **1972**, *35*, 233–246.
- Benkovic, S. J.; Dunikoski, L. K., Jr. *J. Am. Chem. Soc.* **1971**, *93*, 1526–1527.
- Fukui, K.; Morokuma, K.; Nagata, C. *Bull. Chem. Soc. Jpn.* **1960**, *33*, 1214–1219.
- Fukui, K.; Imamura, A.; Nagata, C. *Bull. Chem. Soc. Jpn.* **1963**, *36*, 1450–1453.
- Akola, J.; Jones, R. O. *J. Phys. Chem. B* **2003**, *107*, 11774–11783.
- Frisch, M. J.; Trucks, G. W.; Schlegel, H. B.; Scuseria, G. E.; Robb, M. A.; Cheeseman, J. R.; Montgomery, J. A., Jr.; Vreven, T.; Kudin, K. N.; Burant, J. C.; Millam, J. M.; Iyengar, S. S.; Tomasi, J.; Barone, V.; Mennucci, B.; Cossi, M.; Scalmani, G.; Rega, N.; Petersson, G. A.; Nakatsuji, H.; Hada, M.; Ehara, M.; Toyota, K.; Fukuda, K.; Hasegawa, J.; Ishida, M.; Nakajima, T.; Honda, Y.; Kitao, O.; Nakai, H.; Klene, M.; Li, X.; Knox, J. E.; Hratchian, H. P.; Cross, J. B.; Adamo, C.; Jaramillo, J.; Gomperts, R.; Stratmann, R. E.; Yazyev, O.; Austin, A. J.; Cammi, R.; Pomelli, C.; Ochterski, J. W.; Ayala, P. Y.; Morokuma, K.; Voth, G. A.; Salvador, P.; Dannenberg, J. J.; Zakrzewski, V. G.; Dapprich, S.; Daniels, A. D.; Strain, M. C.; Farkas, O.; Malick, D. K.; Rabuck, A. D.; Raghavachari, K.; Foresman, J. B.; Ortiz, J. V.; Cui, Q.; Baboul, A. G.; Clifford, S.; Cioslowski, J.; Stefanov, B. B.; Liu, G.; Liashenko, A.; Piskorz, P.; Komaromi, I.; Martin, R. L.; Fox, D. J.; Keith, T.; Al-Laham, M. A.; Peng, C. Y.; Nanayakkara, A.; Challacombe, M. W.; Gill, P. M.; Johnson, B.; Chen, W.; Wong, M. W.; Gonzalez, C.; Pople, J. A. *Gaussian03*, revision B.03; Gaussian Inc.: Pittsburgh, PA, 2003.
- Bader, R. F. W. AIMPAC (<http://www.chemistry.mcmaster.ca/aimpac/>).
- Keith, T. A. AIMALL97 (for DOS/Windows) (aim@tkgristmill.com), 2007.
- Biegler-König, F. W.; Bader, R. F. W.; Tang, T.-H. *J. Comput. Chem.* **1982**, *13*, 317–328.
- Zavitsas, A. A. *J. Phys. Chem. A* **2003**, *107*, 897–898.
- Politzer, P.; Habibollahzadeh, D. *J. Chem. Phys.* **1993**, *98*, 7659–7660.
- Hammond, G. S. *J. Am. Chem. Soc.* **1955**, *77*, 334–338.
- Keith, T. A. To be published.
- Löwdin, P.-O. *J. Mol. Spectrosc.* **1959**, *3*, 46–66.
- Magnoli, D. E.; Murdoch, J. R. *Int. J. Quantum Chem.* **1982**, *22*, 1249–1262.
- Kohn, W.; Sham, L. *J. Phys. Rev. A* **1965**, *140* (4A), 1133–1138.
- Becke, A. D. *Phys. Rev. A* **1988**, *38*, 3098–3100.
- Becke, A. *J. Chem. Phys.* **1993**, *98*, 1372–1377.
- Nagy, A. *Phys. Rev. A* **1992**, *46*, 5417–5419.
- Levy, M.; Perdew, J. P. *Phys. Rev. A* **1985**, *32*, 2010–2021.
- Sule, P. *Chem. Phys. Lett.* **1996**, *259*, 69–80.